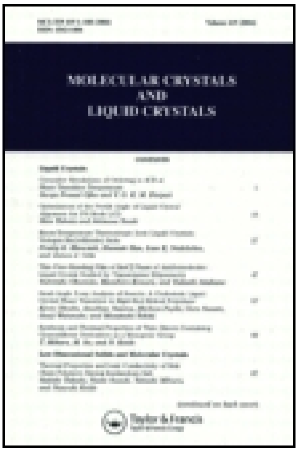

Molecular Crystals and Liquid Crystals
Publication details, including instructions for authors and subscription information:
http://www.tandfonline.com/loi/gmcl20

Effects of Polymer Anchoring on Nematic Liquid Crystals at Nanostructured Polymeric Surfaces

Xuan Zhou [a b] , Zhidong Zhang [c] & Li Xuan [a b]

[a] State Key Lab of Applied Optics, Changchun Institute of Optics, Fine Mechanics and Physics, Chinese Academy of Sciences, Changchun, P. R. China

[b] Graduate School of the Chinese Academy of Sciences, Beijing, P. R. China

[c] Department of Physics, Hebei University of Technology, Tianjin, P. R. China

Version of record first published: 30 Jul 2012.

To cite this article: Xuan Zhou , Zhidong Zhang & Li Xuan (2012): Effects of Polymer Anchoring on Nematic Liquid Crystals at Nanostructured Polymeric Surfaces, Molecular Crystals and Liquid Crystals, 562:1, 85-97

To link to this article: http://dx.doi.org/10.1080/10426507.2012.673846

Mol. Cryst. Liq. Cryst., Vol. 562: pp. 85–97, 2012

ISSN: 1542-1406 print/1563-5287 online
DOI: 10.1080/10426507.2012.673846

Effects of Polymer Anchoring on Nematic Liquid Crystals at Nanostructured Polymeric Surfaces

XUAN ZHOU,[1,2] ZHIDONG ZHANG,[3,*] AND LI XUAN[1,2]

[1]State Key Lab of Applied Optics, Changchun Institute of Optics, Fine Mechanics and Physics, Chinese Academy of Sciences, Changchun, P. R. China
[2]Graduate School of the Chinese Academy of Sciences, Beijing, P. R. China
[3]Department of Physics, Hebei University of Technology, Tianjin, P. R. China

A simplified model of the nanostructured polymeric surface was proposed, characterized by a one-dimensional periodic stripe patterned surface with alternate planar and homeotropic anchoring. We investigate the effect of both the coupling of nematic liquid crystals with alignment layer polymers and the coupling of the polymers with the substrate surface on the anchoring of nematic liquid crystals at such a surface using the extended anisotropic surface energy form proposed by Alexe-Ionescu et al. In our theoretical treatment, we assume the equal anchoring strength of the two anchoring regions. Our results show that the coupling of the polymer with the surface will affect the director field of the nematic, and reduce the relaxation distance as well as the total free energy of the system.

Keywords Director distribution; nanostructured surface; pretilt angle; surface anchoring

Introduction

In liquid crystals (LCs), surface effects have been studied mainly for the nematic phase [1]. The translational symmetry and often the rotational symmetry of the nematic phase are broken when it encounters an interface [2]. In the absence of an external electric or magnetic field (field free condition), the alignment of nematic liquid crystals (NLCs) is entirely dictated by the surface forces, which depends on the presence of surface layers [3]. In the special case where the surface layer is an ordered medium particular effects are expected, because in addition to the physicochemical interactions, the steric interaction also has to be taken into account [4–6]. If the surface layer is polymeric film, the LC molecules are aligned by the sterical interactions between the polymer molecules with the LC molecules [7].

Recently, the nanostructured polymeric layers proposed by Hoi-Sing Kwok et al. seem very promising for application in display technology because they allow a continuous control of the pretilt angle of NLCs [8–10]. The basic idea of the new alignment layer is to form a random distribution of nanosize domains of homogeneous and vertical alignment materials that impart either vertical (V) or horizontal (H) alignment to the LC molecules. Provided that these domains are small, the LC molecules will relax to a uniform pretilt angle

*Address correspondence to Zhidong Zhang, Department of Physics, Hebei University of Technology, Tianjin 300401, P. R. China. E-mail: zhidong_zhang@yahoo.cn

at a short distance above the alignment layer, and this distance is defined as the relaxation distance. It has been shown that such surfaces can have excellent anchoring energies as well as good thermal stability. With the availability of large pretilt angles, many fast response and bistable structures become possible [10,11].

Hoi-Sing Kwok et al. have calculated the director field of an NLC with a one-dimensional (1D) inhomogeneous nanostructured polymeric surface model numerically [9,10], based on the commonly used phenomenological surface anchoring form proposed by Rapini-Papoular (RP) [12]. Their results show that the final pretilt angle depends on the area ratio of the V and H domains, the relative anchoring strengths of the domains as well as the elastic constants of the LC. In addition, the relaxation distance is determined by the size of nanodomains.

Alexe-Ionescu et al. [13] have investigated the anchoring of a polymeric layer consisting of mixed H (mesogenic side groups) and V (aliphatic chains) alignment materials for an NLC sample with homogeneous substrate. They have assumed an extended expression of the anisotropic surface energy for this special surface by considering both the coupling of nematic with alignment layer polymers and the coupling of the polymers with the surface. Their results show that the equivalent anchoring energy can be controlled by controlling the anchoring strength of H and V alignment materials. However, their homogeneous surface is different from the nanostructured model of Hoi-Sing Kwok et al., moreover, their method of polymers blends and co-polymers (mixing H and V alignment materials together) as the alignment layer cannot realize the continuous control of the pretilt angle experimentally.

Nematic samples in contact with 1D periodic patterned surfaces with alternate planar and homeotropic stripes, which are similar to the 1D nanostructured model of Hoi-Sing Kwok et al. [9,10], have received much theoretical [14–16] and experimental attention [17,18]. Atherton et al. [14] have investigated the orientational transition in an NLC with such a surface, in order to get the analytic solutions of the director distribution, they have proposed a Fourier series solution of the director field and assumed the equal anchoring strength of the two regions. Their theoretical results can explain the numerical results of Hoi-Sing Kwok et al. [9,10] in a sense of the RP description of the surface anchoring. However, neither Atherton's nor Hoi-Sing Kwok's study have taken into account the coupling of the polymer with the surface.

In this paper, extending the work of Atherton et al. [14], we investigate the anchoring of an NLC with nanostructured polymeric layers. In our theoretical treatment, we adopt the similar assumption as that used by Atherton et al., i.e., the anchoring strength of the two regions are equal to get the analytic solutions of the director distribution. Then, we analyze the effect of the coupling of the polymer with the surface on NLCs.

Model

Considering a nanostructured surface consisting of regular V and H alignment domains with a common preferred azimuthal direction ϕ, we set up a simplified model of this nanostructured surface characterized by a periodic stripe pattern of period λ along the x-axis, with V domain width $a\lambda$ $(0 < a < 1)$ (see Fig. 1). We choose the z-axis normal to the surface and the y-axis along the stripes. The anchoring on the stripe $0 \leq x < a\lambda$ is homeotropic, whereas the anchoring on the stripe $a\lambda \leq x < \lambda$ is homogeneous planar along the x direction. Due to the translational invariance in the y direction, the director $\vec{n}$ depends only on x and z. Moreover, we assume that the director is confined to the $x - z$

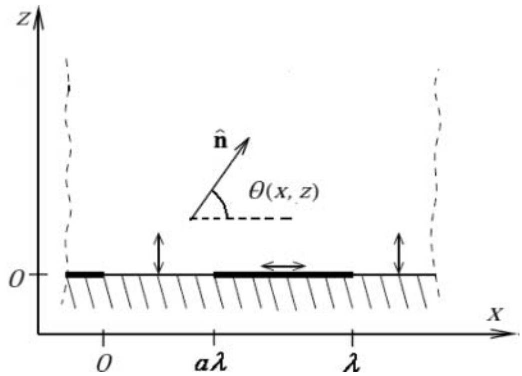

Figure 1. Schematic picture of the model. A periodically patterned surface with period λ. The V domain width $a\lambda$ (thin line), and H domain width $(1 - a)\lambda$ (thick line). The director $\vec{n}$ is confined to the $x - z$ plane.

plane (assuming the azimuthal ϕ alignment to be $//x$), thus, $\vec{n}$ can be written as

$$\vec{n} = (\cos\theta, 0, \sin\theta)\,, \tag{1}$$

where $\theta = \theta(x, z)$.

The final configuration of the namatic is that which minimizes the total free energy including bulk and surface contributions. The bulk energy density is the well-known Frank elastic energy

$$f_b = \frac{1}{2}\left[K_1 (\nabla \cdot \vec{n})^2 + K_2 (\vec{n} \cdot \nabla \times \vec{n})^2 + K_3 (\vec{n} \times \nabla \times \vec{n})^2\right], \tag{2}$$

where K_1, K_2, K_3 are the elastic constants associated with splay, twist, and bend distortions, respectively. The surface-like term $K_s \equiv K_2 + K_{24}$ is omitted here as it does not contribute to the free energy if the director is confined to a single plane. Another surface-like term involving K_{13} is not considered here [19].

The extended anisotropic surface energy density of samples with polymer layers is given by

$$f_{sH} = \frac{1}{2}\alpha_H \sin(\theta^0 - \theta_p)^2 + \frac{1}{2}\beta_H \sin(\theta_p - \theta_e)^2 \tag{3a}$$

for the H domains, and

$$f_{sV} = \frac{1}{2}\alpha_V \sin(\theta^0 - \theta_p)^2 + \frac{1}{2}\beta_V \sin(\theta_p - \theta_e)^2 \tag{3b}$$

for the V domains, where θ_p and θ_e are the direction and easy direction of the polymeric alignment materials, respectively, and θ^0 is the orientation of the director at the surface. The parameters β_H, β_V are connected with the restoring torque of elastic origin acting on the H and V alignment materials, respectively. The parameters α_H, α_V take into account the tendency of the nematic molecules to be parallel, for steric reasons, to the H and V alignment materials, respectively.

To evaluate the free energy, both coordinates are scaled by the period of the nanodomains λ, i.e., $\tilde{x} = \frac{x}{\lambda}$, $\tilde{z} = \frac{z}{\lambda}$. For most nematics $K_2 < K_1 \leq K_3$ [20,21] we, therefore, make the simplification that $K_1 = K_3 = K$. Thus, the bulk free energy density is

$$f_b/K = \frac{1}{2}[(\theta_{,\tilde{x}})^2 + (\theta_{,\tilde{z}})^2]/\lambda^2, \tag{4}$$

where $\theta_{,\tilde{x}} = \partial\theta/\partial\tilde{x}$, $\theta_{,\tilde{z}} = \partial\theta/\partial\tilde{z}$. The Euler-Lagrange equation is

$$\theta_{,\tilde{x}\tilde{x}} + \theta_{,\tilde{z}\tilde{z}} = 0, \tag{5}$$

which has a Fourier series solution that is regular as $z \to \infty$

$$\theta(\tilde{x}, \tilde{z}) = \theta_0 + 2\sum_{n=1}^{\infty} \exp(-2n\pi\tilde{z})\left[p_n \sin(2n\pi\tilde{x}) + q_n \cos(2n\pi\tilde{x})\right]. \tag{6}$$

The coefficients θ_0, p_n, and q_n are to be determined from the total elastic energy minimization, and θ_0 is the final pretilt angle. Substituting Eq. (6) into (4) and integrating over $\tilde{x}$ and $\tilde{z}$ yields the bulk free energy per period

$$F_b/k = 2\pi \sum_{n=1}^{\infty} n\left(p_n^2 + q_n^2\right). \tag{7}$$

In the case $(\theta^0 - \theta_p)$ and $(\theta_p - \theta_e)$ are very small, where Eqs. (3a) and (3b) can be linearized, thus, the surface energy per period is

$$\begin{aligned} F_s/K = &\int_0^a \left[\frac{\lambda}{2L_{\alpha V}}\left[\theta^0(\tilde{x}) - \theta_p(\tilde{x})\right]^2 + \frac{\lambda}{2L_{\beta V}}\left[\theta_p(\tilde{x}) - \theta_e(\tilde{x})\right]^2\right] d\tilde{x} \\ &+ \int_a^1 \left[\frac{\lambda}{2L_{\alpha H}}\left[\theta^0(\tilde{x}) - \theta_p(\tilde{x})\right]^2 + \frac{\lambda}{2L_{\beta H}}\left[\theta_p(\tilde{x}) - \theta_e(\tilde{x})\right]^2\right] d\tilde{x}, \end{aligned} \tag{8}$$

where $L_{\alpha V} = K/\alpha_V$, $L_{\beta V} = K/\beta_V$, $L_{\alpha H} = K/\alpha_H$, $L_{\beta H} = K/\beta_H$, which have the dimension of length and can be defined as the generalized extrapolation lengths for the two domains.

Results

According to the nanostructured surface model above (see Fig. 1), we have

$$\theta_e(\tilde{x}) = \theta_e(\tilde{x} + L) = \begin{cases} \dfrac{\pi}{2} & 0 \leq \tilde{x} < a \\ 0 & a \leq \tilde{x} < 1 \end{cases}, \tag{9}$$

with L being an arbitrary integer. The periodic function $\theta_e(x)$ can be approximately written as Fourier series form, that is

$$\theta_e(\tilde{x}) = \frac{\pi}{2}a + 2\sum_{n=1}^{\infty}\left[\frac{\sin^2(n\pi a)}{2n}\sin(2n\pi\tilde{x}) + \frac{\sin(2n\pi a)}{4n}\cos(2n\pi\tilde{x})\right]. \tag{10}$$

As θ_p and θ are also periodic functions along x direction, we can assume

$$\theta_p(\tilde{x}) = \theta_0{}' + 2\sum_{n=1}^{\infty}\left[p_n'\sin(2n\pi\tilde{x}) + q_n'\cos(2n\pi\tilde{x})\right], \tag{11}$$

$$\theta^0(\tilde{x}) = \theta(\tilde{x}, 0) = \theta_0 + 2\sum_{n=1}^{\infty}\left[p_n\sin(2n\pi\tilde{x}) + q_n\cos(2n\pi\tilde{x})\right]. \tag{12}$$

Substituting Eqs. (10)–(12) into Eq. (8) and integrating, and then combined with the bulk free energy given by Eq. (7), we can get the expression of the total free energy per period $F(\theta_0, \theta_0', p_n, q_n, p_n', q_n'; n = 1, 2, 3\ldots)$.

The coefficients θ_0, θ_0', q_n, p_n and p_n', q_n' have to minimize the function F, that is, $\frac{\partial F}{\partial \theta_0} = \frac{\partial F}{\partial \theta_0'} = 0$, $\frac{\partial F}{\partial p_n} = \frac{\partial F}{\partial q_n} = \frac{\partial F}{\partial p_n'} = \frac{\partial F}{\partial q_n'} = 0$. These relations constitute a system of linear inhomogeneous equations, which can be written as Matrix-vector form

$$AX = B, \tag{13}$$

where the matrix A and vectors X, B are expressed as

$$A = \begin{bmatrix} A_{11} & A_{12} & \cdots & A_{1,4m-1} & A_{1,4m} & A_{1,4m+1} & A_{1,4m+2} & \cdots \\ A_{21} & A_{22} & \cdots & A_{2,4m-1} & A_{2,4m} & A_{2,4m+1} & A_{2,4m+2} & \cdots \\ \vdots & \vdots & \vdots & \vdots & \vdots & \vdots & \vdots & \vdots \\ A_{4n-1,1} & A_{4n-1,2} & \cdots & A_{4n-1,4m-1} & A_{4n-1,4m} & A_{4n-1,4m+1} & A_{4n-1,4m+2} & \cdots \\ A_{4n,1} & A_{4n,2} & \cdots & A_{4n,4m-1} & A_{4n,4m} & A_{4n,4m+1} & A_{4n,4m+2} & \cdots \\ A_{4n+1,1} & A_{4n+1,2} & \cdots & A_{4n+1,4m-1} & A_{4n+1,4m} & A_{4n+1,4m+1} & A_{4n+1,4m+2} & \cdots \\ A_{4n+2,1} & A_{4n+2,2} & \cdots & A_{4n+2,4m-1} & A_{4n+2,4m} & A_{4n+2,4m+1} & A_{4n+2,4m+2} & \cdots \\ \vdots & \vdots & \vdots & \vdots & \vdots & \vdots & \vdots & \vdots \end{bmatrix}$$

$$(n, m = 1, 2, \ldots), \tag{14}$$

$$X = \left[X_1\ X_2\ \cdots\ X_{4m-1}\ X_{4m}\ X_{4m+1}\ X_{4m+2}\ \cdots\right]^{\mathrm{T}} \quad (m = 1, 2, \ldots), \tag{15}$$

$$B = \left[B_1\ B_2\ \cdots\ B_{4n-1}\ B_{4n}\ B_{4n+1}\ B_{4n+2}\ \cdots\right]^{\mathrm{T}} \quad (n = 1, 2, \ldots). \tag{16}$$

Each matrix element of A, X, and B is given in Appendix A.

The expressions given in Appendix A show that the coefficients θ_0, θ_0', q_n, p_n and p_n', q_n' are determined by the parameters a and $L_{\alpha H}$, $L_{\beta H}$, $L_{\alpha V}$, $L_{\beta V}$ (α_H, β_H, α_V, β_V). Equation (6) gives that the final pretilt angle is θ_0, meaning that besides the area ratio of V and H domains, and the coupling of the nematic with the polymer (a, α_H, α_V), which have been verified theoretically and experimentally by Hoi-Sing Kwok et al. [8–10], the coupling of the polymer with the surface (β_H, β_V) also has important contribution to the final pretilt angle. We should notice that the effect of the relative elastic constants does not exist here, that is because we have assumed $K_1 = K_3 = K$.

In order to analyze the effect of the polymer anchoring further, following the treatment method of Atherton et al. [14], we assume $L_{\alpha H} = L_{\alpha V} = L_\alpha$, $L_{\beta H} = L_{\beta V} = L_\beta$, i.e., $\alpha_H = \alpha_V = \alpha$, $\beta_H = \beta_V = \beta$, and then the mathematical structure given by Eq. (13) can be simplified, the details are given in Appendix B. Equations (B7–B9) give the analytical expression of each coefficient

$$\theta_0 = \theta_0' = \frac{\pi a}{2}, \tag{17}$$

$$p_n = \frac{1}{1 + 2n\pi L_e/\lambda} \frac{\sin^2(n\pi a)}{2n}, \tag{18}$$

$$q_n = \frac{1}{1 + 2n\pi L_e/\lambda} \frac{\sin(2n\pi a)}{4n}, \tag{19}$$

$$p_n' = \frac{1 + 2n\pi L_\alpha/\lambda}{1 + 2n\pi L_e/\lambda} \frac{\sin^2(n\pi a)}{2n}, \tag{20}$$

$$q_n' = \frac{1 + 2n\pi L_\alpha/\lambda}{1 + 2n\pi L_e/\lambda} \frac{\sin(2n\pi a)}{4n}, \tag{21}$$

where we have put $L_e = L_\alpha + L_\beta$, defining $L_e = K/w_e$ and combining it with the definition of L_α and L_β, i.e., $L_\alpha = K/\alpha$, $L_\beta = K/\beta$, we can easily get

$$\frac{1}{w_e} = \frac{1}{\alpha} + \frac{1}{\beta}. \tag{22}$$

Comparing Eqs. (18)–(19) with the results given by Atherton et al. [14], i.e.

$$p_n = \frac{1}{1 + 2n\pi L_\alpha/\lambda} \frac{\sin^2(n\pi a)}{2n}, \tag{23}$$

$$q_n = \frac{1}{1 + 2n\pi L_\alpha/\lambda} \frac{\sin(2n\pi a)}{4n}, \tag{24}$$

we find that, in the consideration of the coupling of the polymer with the surface, we get an equivalent anchoring energy [see Eq. (22)], which is consistent with that of Alexe-Ionescu et al. [13].

Substituting Eqs. (18)–(19) into Eq. (6), we get

$$\begin{aligned}\theta(\tilde{x}, \tilde{z}) = \frac{\pi a}{2} + 2\sum_{n=1}^{\infty} \exp(-2n\pi\tilde{z}) \frac{1}{1 + 2n\pi L_e/\lambda} \\ \times \left[\frac{\sin^2(n\pi a)}{2n} \sin(2n\pi\tilde{x}) + \frac{\sin(2n\pi a)}{4n} \cos(2n\pi\tilde{x})\right].\end{aligned} \tag{25}$$

Equation (25) shows that the coupling of the polymer with the surface affects the tilt angle distribution of the nematic director.

In addition, Eqs. (18)–(21) give the total free energy per period

$$F = \pi K \sum_{n=1}^{\infty} \frac{\sin^2(n\pi a)}{2n} \frac{1}{1 + 2n\pi L_e/\lambda}, \tag{26}$$

and the associated total free energy density

$$F/\lambda = \pi K \sum_{n=1}^{\infty} \frac{\sin^2(n\pi a)}{2n} \frac{1}{\lambda + 2n\pi L_e}. \tag{27}$$

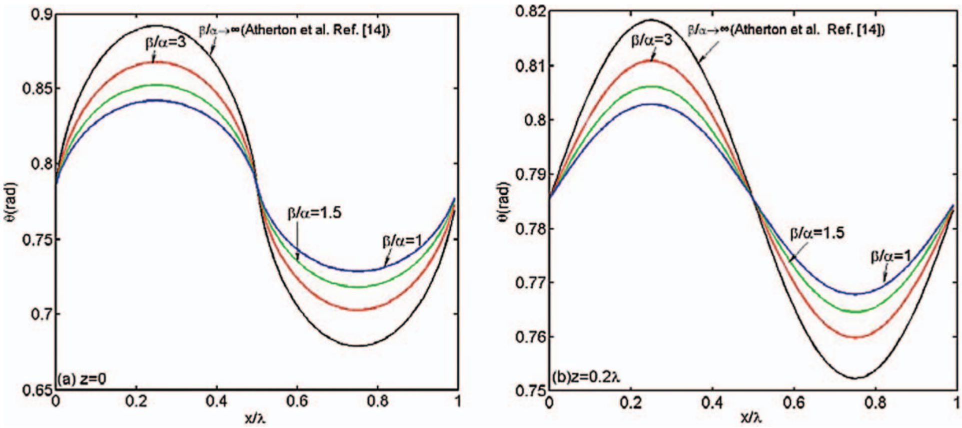

Figure 2. Tilt angle of the nematic director at a certain distance of z as a function of x. We show our present result and that reported in Ref. [14]. (a) $z = 0$; (b) $z = 0.2\lambda$.

Equations (25) and (27) may be used to evaluate the tilt angle of the nematic director and the total free energy density of the system, respectively.

To see the effect of the coupling of the polymer with the surface clearly, we now discuss our result in comparison with that of Atherton et al. [14] by using numerical calculations, with the parameters as follows $K = 1.2 \times 10^{-11} N$, $\lambda = 0.1 um$, and $a = 0.5$.

We plot the x dependence of the tilt angle θ at a certain distance of z for various β/α with $\alpha = 10^{-4} Jm^{-2}$ in Fig. 2, which shows our present result and that reported in Ref. [14]. It is clear that the coupling of the polymer with the surface affects the tilt angle of the nematic director. As the anchoring parameter β increasing, our result tends to that of Atherton et al. [14], which is reasonable. In addition, from Fig. 2, we can conclude that the coupling of the polymer with the surface will reduce the relaxation distance.

The total free energy density of the system F/λ is plotted in Fig. 3 as a function of α for several values of β. We find that the coupling of the polymer with the surface reduces

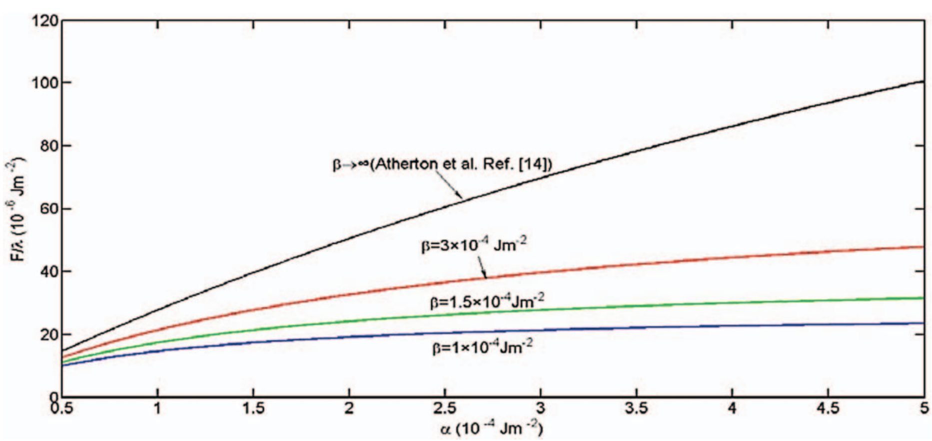

Figure 3. The α dependence of the total free energy density F/λ for various β. We show the present theoretical result and that reported in Ref. [14].

the total free energy of the system. As the anchoring parameter β increasing, our result tends to that of Atherton et al. [14].

Conclusions

In this work, extending the work of Atherton et al., we have set up a simplified model of the nanostructured polymeric surface, characterized by a 1D periodic stripe patterned surface with alternate planar and homeotropic anchoring, and investigated the effect of both the coupling of nematic with alignment layer polymers and the coupling of the polymers with the substrate surface on the anchoring of an NLC at such a surface. Our results confirm the results reported by Hoi-Sing Kwok et al. [8–10]. By assuming the equal anchoring strength of the two regions and comparing with the results of Atherton et al. [14], we get the same equivalent anchoring energy w_e [Eq. (22)] to that reported by Alexe-Ionescu et al. [13]. In addition, we find that the coupling of the polymer with the surface will affect the director field of the nematic, and reduce the relaxation distance as well as the total free energy of the system.

Acknowledgments

This research was supported by Natural Science Foundation of Hebei Province under Grant No. A2010000004 and National Natural Science Foundation of China under Grants No. 60736042, and Key Subject Construction Project of Hebei Province University.

References

[1] Jérome, B. (1991). *Rep. Prog. Phys.*, *54*, 391.
[2] Barbero, G., Gabbasova, Z., & Osipov, M. A. (1991). *J. Phys. France*, *1*, 691.
[3] Blinov, L. M., & Chigrinov, V. G. (1994). *Electrooptic Effects in Liquid Crystal Materials*, Springer-Verlag: New York.
[4] Barbero, G., & Petrov, A. G. (1994). *J. Phys.: Condens. Matter*, *6*, 2291.
[5] Fazio, V. S. U., Nannelli, F., & Komitov, L. (2001). *Phys. Rev. E*, *63*, 061712, 1–8.
[6] Ferrer, F. J., Frutos, F., García-López, F. J., González-Elipe, A. R., & Yubero, F. (2007). *Thin Solid Films*, *516*, 481.
[7] Patel, J. S., Leslie, T. M., & Goodby, J. W. (1984). *Ferroelectrics*, *59*, 137.
[8] Yeung, F. S., Ho, J. Y., Li, Y. W., Xie, F. C., Tsui, O. K., Sheng, P., & Kwok, H. S. (2006). *Appl. Phys. Lett.*, *88*, 051910, 1–3.
[9] Yeung, F. S., Xie, F. C., Wan, J., Lee, F. K., Tsui, O. K., Sheng, P., & Kwok, H. S. (2006). *J. Appl. Phys.*, *99*, 124506, 1–4.
[10] Yeung, F. S., Xie, F. C., Kwok, H. S., Wan, J., Tsui, O. K., & Sheng, P. (2005). *SID05 Digest*, *36*, 1080.
[11] Yeung, F. S., & Tsui, O. K. (2006). *Appl. Phys. Lett.*, *88*, 063505, 1–3.
[12] Rapini, A., & Papoular, M. (1969). *J. Phys. (Paris) Colloq.*, *30*, C4.
[13] Alexe-Ionescu, A. L., Barbero, G., & Komitov, L. (2008). *Phys. Rev. E*, *77*, 051701, 1–8.
[14] Atherton, T. J., & Sambles, J. R. (2006). *Phys. Rev. E*, *74*, 022701, 1–4.
[15] Kondrat, S., & Poniewierski, A. (2001). *Phys. Rev. E*, *64*, 31709.
[16] Barbero, G., Beica, T., Alexe-Ionescu, A. L., & Moldovan, R. (1992). *J. Phys. France*, *2*, 2011.
[17] Schadt, M., Seiberle, H., & Schuster, A. (1996). *Nature*, *381*, 212.
[18] Gupta, V. K., & Abbot, N. L. (1997). *Science*, *276*, 1533.
[19] Yokoyama, H. (1997). *Phys. Rev. E*, *55*, 2938.
[20] Pieranski, P., Brochard, F., & Guyon, E. (1972). *J. Phys. France*, *33*, 681.
[21] Wahl, J., & Fisher, F. (1973). *Mol. Cryst. Liq. Cryst.*, *22*, 359.

Appendix A: The Expression of Each Matrix Element

From the calculated total free energy $F\left(\theta_0, \theta_0', p_n, q_n, p_n', q_n'; n = 1, 2, 3\cdots\right)$ and the relations $\frac{\partial F}{\partial \theta_0} = \frac{\partial F}{\partial \theta_0'} = 0$, $\frac{\partial F}{\partial p_n} = \frac{\partial F}{\partial q_n} = \frac{\partial F}{\partial p_n'} = \frac{\partial F}{\partial q_n'} = 0$, we have

$$A_{11} = \frac{\lambda}{L_{\alpha H}}(1-a) + \frac{\lambda}{L_{\alpha V}}a, \tag{A1a}$$

$$A_{22} = \left[\frac{\lambda}{L_{\alpha H}}(1-a) + \frac{\lambda}{L_{\alpha V}}a\right] + \left[\frac{\lambda}{L_{\beta H}}(1-a) + \frac{\lambda}{L_{\beta V}}a\right], \tag{A1b}$$

$$A_{12} = A_{21} = -\left[\frac{\lambda}{L_{\alpha H}}(1-a) + \frac{\lambda}{L_{\alpha V}}a\right]. \tag{A1c}$$

$$A_{1,4m-1} = -\left(\frac{2\lambda}{L_{\alpha H}} - \frac{2\lambda}{L_{\alpha V}}\right)\frac{\sin^2(m\pi a)}{m\pi}, \tag{A2a}$$

$$A_{1,4m} = -\left(\frac{2\lambda}{L_{\alpha H}} - \frac{2\lambda}{L_{\alpha V}}\right)\frac{\sin(2m\pi a)}{2m\pi}, \tag{A2b}$$

$$A_{1,4m+1} = A_{2,4m-1} = \left(\frac{2\lambda}{L_{\alpha H}} - \frac{2\lambda}{L_{\alpha V}}\right)\frac{\sin^2(m\pi a)}{m\pi}, \tag{A2c}$$

$$A_{1,4m+2} = A_{2,4m} = \left(\frac{2\lambda}{L_{\alpha H}} - \frac{2\lambda}{L_{\alpha V}}\right)\frac{\sin(2m\pi a)}{2m\pi}, \tag{A2d}$$

$$A_{2,4m+1} = -\left[\left(\frac{2\lambda}{L_{\alpha H}} - \frac{2\lambda}{L_{\alpha V}}\right) + \left(\frac{2\lambda}{L_{\beta H}} - \frac{2\lambda}{L_{\beta V}}\right)\right]\frac{\sin^2(m\pi a)}{m\pi}, \tag{A2e}$$

$$A_{2,4m+2} = -\left[\left(\frac{2\lambda}{L_{\alpha H}} - \frac{2\lambda}{L_{\alpha V}}\right) + \left(\frac{2\lambda}{L_{\beta H}} - \frac{2\lambda}{L_{\beta V}}\right)\right]\frac{\sin(2m\pi a)}{2m\pi}. \tag{A2f}$$

$$A_{4n-1,1} = -\left(\frac{2\lambda}{L_{\alpha H}} - \frac{2\lambda}{L_{\alpha V}}\right)\frac{\sin^2(n\pi a)}{n\pi}, \tag{A3a}$$

$$A_{4n-1,2} = A_{4n+1,1} = \left(\frac{2\lambda}{L_{\alpha H}} - \frac{2\lambda}{L_{\alpha V}}\right)\frac{\sin^2(n\pi a)}{n\pi}, \tag{A3b}$$

$$A_{4n,1} = -\left(\frac{2\lambda}{L_{\alpha H}} - \frac{2\lambda}{L_{\alpha V}}\right)\frac{\sin(2n\pi a)}{2n\pi}, \tag{A3c}$$

$$A_{4n,2} = A_{4n+2,1} = \left(\frac{2\lambda}{L_{\alpha H}} - \frac{2\lambda}{L_{\alpha V}}\right)\frac{\sin(2n\pi a)}{2n\pi}, \tag{A3d}$$

$$A_{4n+1,2} = -\left[\left(\frac{2\lambda}{L_{\alpha H}} - \frac{2\lambda}{L_{\alpha V}}\right) + \left(\frac{2\lambda}{L_{\beta H}} - \frac{2\lambda}{L_{\beta V}}\right)\right]\frac{\sin^2(n\pi a)}{n\pi}, \tag{A3e}$$

$$A_{4n+2,2} = -\left[\left(\frac{2\lambda}{L_{\alpha H}} - \frac{2\lambda}{L_{\alpha V}}\right) + \left(\frac{2\lambda}{L_{\beta H}} - \frac{2\lambda}{L_{\beta V}}\right)\right]\frac{\sin(2n\pi a)}{2n\pi}. \tag{A3f}$$

When $n = m$, we have

$$A_{4n-1,4n-1} = 4n\pi + \frac{2\lambda}{L_{\alpha H}}\left(1 - a + \frac{\sin(4n\pi a)}{4n\pi}\right) + \frac{2\lambda}{L_{\alpha V}}\left(a - \frac{\sin(4n\pi a)}{4n\pi}\right), \quad \text{(A4a)}$$

$$A_{4n,4n} = 4n\pi + \frac{2\lambda}{L_{\alpha H}}\left(1 - a - \frac{\sin(4n\pi a)}{4n\pi}\right) + \frac{2\lambda}{L_{\alpha V}}\left(a + \frac{\sin(4n\pi a)}{4n\pi}\right), \quad \text{(A4b)}$$

$$A_{4n+1,4n+1} = \frac{2\lambda}{L_{\alpha H}}\left(1 - a + \frac{\sin(4n\pi a)}{4n\pi}\right) + \frac{2\lambda}{L_{\alpha V}}\left(a - \frac{\sin(4n\pi a)}{4n\pi}\right) + \frac{2\lambda}{L_{\beta H}}\left(1 - a + \frac{\sin(4n\pi a)}{4n\pi}\right) + \frac{2\lambda}{L_{\beta V}}\left(a - \frac{\sin(4n\pi a)}{4n\pi}\right), \quad \text{(A4c)}$$

$$A_{4n+2,4n+2} = \frac{2\lambda}{L_{\alpha H}}\left(1 - a - \frac{\sin(4n\pi a)}{4n\pi}\right) + \frac{2\lambda}{L_{\alpha V}}\left(a + \frac{\sin(4n\pi a)}{4n\pi}\right) + \frac{2\lambda}{L_{\beta H}}\left(1 - a - \frac{\sin(4n\pi a)}{4n\pi}\right) + \frac{2\lambda}{L_{\beta V}}\left(a + \frac{\sin(4n\pi a)}{4n\pi}\right), \quad \text{(A4d)}$$

$$A_{4n-1,4n+1} = A_{4n+1,4n-1} = -\left[\frac{2\lambda}{L_{\alpha H}}\left(1 - a + \frac{\sin(4n\pi a)}{4n\pi}\right) + \frac{2\lambda}{L_{\alpha V}}\left(a - \frac{\sin(4n\pi a)}{4n\pi}\right)\right], \quad \text{(A4e)}$$

$$A_{4n,4n+2} = A_{4n+2,4n} = -\left[\frac{2\lambda}{L_{\alpha H}}\left(1 - a - \frac{\sin(4n\pi a)}{4n\pi}\right) + \frac{2\lambda}{L_{\alpha V}}\left(a + \frac{\sin(4n\pi a)}{4n\pi}\right)\right], \quad \text{(A4f)}$$

$$A_{4n-1,4n} = A_{4n-1,4n+2} = A_{4n,4n-1} = A_{4n,4n+1} = A_{4n+1,4n} = A_{4n+1,4n+2} = A_{4n+2,4n-1} = A_{4n+2,4n+1} = 0. \quad \text{(A4g)}$$

When $n \neq m$

$$A_{4n-1,4m-1} = \left(\frac{2\lambda}{L_{\alpha H}} - \frac{2\lambda}{L_{\alpha V}}\right)\left[\frac{\sin(2n+2m)\pi a}{(2n+2m)\pi} - \frac{\sin(2n-2m)\pi a}{(2n-2m)\pi}\right], \quad \text{(A5a)}$$

$$A_{4n-1,4m} = -\left(\frac{2\lambda}{L_{\alpha H}} - \frac{2\lambda}{L_{\alpha V}}\right)\left[\frac{\sin^2(n+m)\pi a}{(n+m)\pi} + \frac{\sin^2(n-m)\pi a}{(n-m)\pi}\right], \quad \text{(A5b)}$$

$$A_{4n-1,4m+1} = A_{4n+1,4m-1} = -\left(\frac{2\lambda}{L_{\alpha H}} - \frac{2\lambda}{L_{\alpha V}}\right) \times \left[\frac{\sin(2n+2m)\pi a}{(2n+2m)\pi} - \frac{\sin(2n-2m)\pi a}{(2n-2m)\pi}\right], \quad \text{(A5c)}$$

$$A_{4n-1,4m+2} = A_{4n+1,4m} = -\left(\frac{2\lambda}{L_{\alpha H}} - \frac{2\lambda}{L_{\alpha V}}\right) \times \left[\frac{\sin^2(n+m)\pi a}{(n+m)\pi} + \frac{\sin^2(n-m)\pi a}{(n-m)\pi}\right], \quad \text{(A5d)}$$

$$A_{4n,4m-1} = -\left(\frac{2\lambda}{L_{\alpha H}} - \frac{2\lambda}{L_{\alpha V}}\right)\left[\frac{\sin^2(n+m)\pi a}{(n+m)\pi} - \frac{\sin^2(n-m)\pi a}{(n-m)\pi}\right], \quad \text{(A5e)}$$

$$A_{4n,4m} = -\left(\frac{2\lambda}{L_{\alpha H}} - \frac{2\lambda}{L_{\alpha V}}\right)\left[\frac{\sin(2n+2m)\pi a}{(2n+2m)\pi} + \frac{\sin(2n-2m)\pi a}{(2n-2m)\pi}\right], \quad \text{(A5f)}$$

$$A_{4n,4m+1} = A_{4n+2,4m-1} = \left(\frac{2\lambda}{L_{\alpha H}} - \frac{2\lambda}{L_{\alpha V}}\right) \times \left[\frac{\sin^2(n+m)\pi a}{(n+m)\pi} - \frac{\sin^2(n-m)\pi a}{(n-m)\pi}\right], \quad \text{(A5g)}$$

$$A_{4n,4m+2} = A_{4n+2,4m} = \left(\frac{2\lambda}{L_{\alpha H}} - \frac{2\lambda}{L_{\alpha V}}\right) \times \left[\frac{\sin(2n+2m)\pi a}{(2n+2m)\pi} + \frac{\sin(2n-2m)\pi a}{(2n-2m)\pi}\right], \quad \text{(A5h)}$$

$$A_{4n+1,4m+1} = \left[\left(\frac{2\lambda}{L_{\alpha H}} - \frac{2\lambda}{L_{\alpha V}}\right) + \left(\frac{2\lambda}{L_{\beta H}} - \frac{2\lambda}{L_{\beta V}}\right)\right] \times \left[\frac{\sin(2n+2m)\pi a}{(2n+2m)\pi} - \frac{\sin(2n-2m)\pi a}{(2n-2m)\pi}\right], \quad \text{(A5i)}$$

$$A_{4n+1,4m+2} = -\left[\left(\frac{2\lambda}{L_{\alpha H}} - \frac{2\lambda}{L_{\alpha V}}\right) + \left(\frac{2\lambda}{L_{\beta H}} - \frac{2\lambda}{L_{\beta V}}\right)\right] \times \left[\frac{\sin^2(n+m)\pi a}{(n+m)\pi} + \frac{\sin^2(n-m)\pi a}{(n-m)\pi}\right], \quad \text{(A5j)}$$

$$A_{4n+2,4m+1} = -\left[\left(\frac{2\lambda}{L_{\alpha H}} - \frac{2\lambda}{L_{\alpha V}}\right) + \left(\frac{2\lambda}{L_{\beta H}} - \frac{2\lambda}{L_{\beta V}}\right)\right] \times \left[\frac{\sin^2(n+m)\pi a}{(n+m)\pi} - \frac{\sin^2(n-m)\pi a}{(n-m)\pi}\right], \quad \text{(A5k)}$$

$$A_{4n+2,4m+2} = -\left[\left(\frac{2\lambda}{L_{\alpha H}} - \frac{2\lambda}{L_{\alpha V}}\right) + \left(\frac{2\lambda}{L_{\beta H}} - \frac{2\lambda}{L_{\beta V}}\right)\right] \times \left[\frac{\sin(2n+2m)\pi a}{(2n+2m)\pi} + \frac{\sin(2n-2m)\pi a}{(2n-2m)\pi}\right]. \quad \text{(A5l)}$$

$$X_1 = \theta_0,\ X_2 = \theta_0',\ X_{4m-1} = p_m,\ X_{4m} = q_m,\ X_{4m+1} = p_m',\ X_{4m+2} = q_m'. \quad \text{(A6)}$$

$$B_1 = B_{4n-1} = B_{4n} = 0, \quad \text{(A7a)}$$

$$B_2 = \left[\frac{\lambda}{L_{\beta H}}(1-a) + \frac{\lambda}{L_{\beta V}}a\right] \cdot \frac{\pi}{2}a - \sum_{n=1}^{\infty}\left(\frac{2\lambda}{L_{\beta H}} - \frac{2\lambda}{L_{\beta V}}\right)\frac{\sin^2(n\pi a)}{n^2\pi}, \quad \text{(A7b)}$$

$$B_{4n+1} = \left[\frac{\lambda}{L_{\beta H}}\left(1 - a + \frac{\sin(4n\pi a)}{4n\pi}\right) + \frac{\lambda}{L_{\beta V}}\left(a - \frac{\sin(4n\pi a)}{4n\pi}\right)\right]\frac{\sin^2(n\pi a)}{n} + \sum_{m\neq n}\left(\frac{\lambda}{L_{\beta H}} - \frac{\lambda}{L_{\beta V}}\right)\left[\frac{\sin(2n+2m)\pi a}{(2n+2m)\pi} - \frac{\sin(2n-2m)\pi a}{(2n-2m)\pi}\right]\frac{\sin^2(m\pi a)}{m}$$

$$-\sum_{m\neq n}\left(\frac{\lambda}{L_{\beta H}}-\frac{\lambda}{L_{\beta V}}\right)\left[\frac{\sin^2(n+m)\pi a}{(n+m)\pi}+\frac{\sin^2(n-m)\pi a}{(n-m)\pi}\right]\frac{\sin(2m\pi a)}{2m}, \quad \text{(A7c)}$$

$$B_{4n+2}=\left[\frac{\lambda}{L_{\beta H}}\left(1-a-\frac{\sin(4n\pi a)}{4n\pi}\right)+\frac{\lambda}{L_{\beta V}}\left(a+\frac{\sin(4n\pi a)}{4n\pi}\right)\right]\frac{\sin(2n\pi a)}{2n}$$

$$-\sum_{m\neq n}\left(\frac{\lambda}{L_{\beta H}}-\frac{\lambda}{L_{\beta V}}\right)\left[\frac{\sin(2n+2m)\pi a}{(2n+2m)\pi}+\frac{\sin(2n-2m)\pi a}{(2n\mp 2m)\pi}\right]\frac{\sin(2m\pi a)}{m}$$

$$-\sum_{m\neq n}\left(\frac{\lambda}{L_{\beta H}}-\frac{\lambda}{L_{\beta V}}\right)\left[\frac{\sin^2(n+m)\pi a}{(n+m)\pi}-\frac{\sin^2(n-m)\pi a}{(n-m)\pi}\right]\frac{\sin^2(m\pi a)}{m}. \quad \text{(A7d)}$$

Appendix B The Simplified Expression of Each Matrix Element

On the assumption of $L_{\alpha H}=L_{\alpha V}=L_\alpha$, $L_{\beta H}=L_{\beta V}=L_\beta$ from the expressions given in Appendix A, we can easily get

$$A_{11}=\frac{\lambda}{L_\alpha}, \quad \text{(B1a)}$$

$$A_{22}=\frac{\lambda}{L_\alpha}+\frac{\lambda}{L_\beta}, \quad \text{(B1b)}$$

$$A_{12}=A_{21}=-\frac{\lambda}{L_\alpha}. \quad \text{(B1c)}$$

$$A_{1,4m-1}=A_{1,4m}=A_{1,4m+1}=A_{1,4m+2}=A_{2,4m-1}=A_{2,4m}=A_{2,4m+1}=A_{2,4m+2}=0. \quad \text{(B2)}$$

$$A_{4n-1,1}=A_{4n,1}=A_{4n+1,1}=A_{4n+2,1}=A_{4n-1,2}=A_{4n,2}=A_{4n+1,2}=A_{4n+2,2}=0. \quad \text{(B3)}$$

When $n=m$, we have

$$A_{4n-1,4n-1}=A_{4n,4n}=4n\pi+\frac{2\lambda}{L_\alpha}, \quad \text{(B4a)}$$

$$A_{4n+1,4n+1}=A_{4n+2,4n+2}=\frac{2\lambda}{L_\alpha}+\frac{2\lambda}{L_\beta}, \quad \text{(B4b)}$$

$$A_{4n-1,4n+1}=A_{4n+1,4n-1}=A_{4n,4n+2}=A_{4n+2,4n}=-\frac{2\lambda}{L_\alpha}, \quad \text{(B4c)}$$

$$A_{4n-1,4n}=A_{4n-1,4n+2}=A_{4n,4n-1}=A_{4n,4n+1}=A_{4n+1,4n}=A_{4n+1,4n+2}=A_{4n+2,4n-1}=A_{4n+2,4n+1}=0. \quad \text{(B4d)}$$

When $n\neq m$

$$A_{4n-1,4m-1}=A_{4n-1,4m}=A_{4n-1,4m+1}=A_{4n-1,4m+2}=0, \quad \text{(B5a)}$$

$$A_{4n,4m-1}=A_{4n,4m}=A_{4n,4m+1}=A_{4n,4m+2}=0, \quad \text{(B5b)}$$

$$A_{4n+1,4m-1}=A_{4n+1,4m}=A_{4n+1,4m+1}=A_{4n+1,4m+2}=0, \quad \text{(B5c)}$$

$$A_{4n+2,4m-1} = A_{4n+2,4m} = A_{4n+2,4m+1} = A_{4n+,4m+2} = 0. \tag{B5d}$$

$$B_1 = B_{4n-1} = B_{4n} = 0, \tag{B6a}$$

$$B_2 = \frac{\lambda}{L_\beta}\frac{\pi}{2}a, \tag{B6b}$$

$$B_{4n+1} = \frac{\lambda}{L_\beta}\frac{\sin^2(n\pi a)}{n}, \tag{B6c}$$

$$B_{4n+2} = \frac{\lambda}{L_\beta}\frac{\sin(2n\pi a)}{2n}. \tag{B6d}$$

Thus, the mathematical structure $AX = B$ can be simplified to the following equations sets:

$$\begin{cases} \frac{2\lambda}{L_\alpha}\left(\theta_0 - \theta_0'\right) = 0 \\ -\frac{\lambda}{L_\alpha}\theta_0 + \left(\frac{\lambda}{L_\alpha} + \frac{\lambda}{L_\beta}\right)\theta_0' = \frac{\lambda}{L_\beta}\frac{\pi a}{2} \end{cases} \tag{B7}$$

$$\begin{cases} \left(\frac{2\lambda}{L_\alpha} + 4\pi n\right)p_n - \frac{2\lambda}{L_\alpha}p_n' = 0 \\ -\frac{2\lambda}{L_\alpha}p_n + \left(\frac{2\lambda}{L_\alpha} + \frac{2\lambda}{L_\beta}\right)p_n' = \frac{\lambda}{L_\beta}\frac{\sin^2(n\pi a)}{n} \end{cases} \quad (n = 1, 2, \ldots) \tag{B8}$$

$$\begin{cases} \left(\frac{2\lambda}{L_\alpha} + 4\pi n\right)q_n - \frac{2\lambda}{L_\alpha}q_n' = 0 \\ -\frac{2\lambda}{L_\alpha}q_n + \left(\frac{2\lambda}{L_\alpha} + \frac{2\lambda}{L_\beta}\right)q_n' = \frac{\lambda}{L_\beta}\frac{\sin(2n\pi a)}{2n} \end{cases} \quad n = (1, 2, \ldots) \tag{B9}$$